Hindawi
Advances in Civil Engineering
Volume 2020, Article ID 8898126, 12 pages
https://doi.org/10.1155/2020/8898126

Research Article

Assessment for Thermal Conductivity of Frozen Soil Based on Nonlinear Regression and Support Vector Regression Methods

Fu-Qing Cui,[1,2] **Wei Zhang**,[1] **Zhi-Yun Liu**,[1] **Wei Wang**,[1] **Jian-bing Chen**,[2] **Long Jin**,[2] **and Hui Peng**[2]

[1]*College of Geological Engineering and Geomatics, Chang'an University, Xi'an, Shaanxi 710054, China*
[2]*State Key Laboratory of Road Engineering Safety and Health in Cold and High-Altitude Regions, CCCC First Highway Consultants Co. Ltd., Xi'an, Shaanxi 710065, China*

Correspondence should be addressed to Zhi-Yun Liu; dcdgx33@chd.edu.cn

Received 19 July 2020; Revised 5 August 2020; Accepted 19 August 2020; Published 28 August 2020

Academic Editor: Yanjun Shen

The comprehensive understanding of the variation law of soil thermal conductivity is the prerequisite of design and construction of engineering applications in permafrost regions. Compared with the unfrozen soil, the specimen preparation and experimental procedures of frozen soil thermal conductivity testing are more complex and challengeable. In this work, considering for essentially multiphase and porous structural characteristic information reflection of unfrozen soil thermal conductivity, prediction models of frozen soil thermal conductivity using nonlinear regression and Support Vector Regression (SVR) methods have been developed. Thermal conductivity of multiple types of soil samples which are sampled from the Qinghai-Tibet Engineering Corridor (QTEC) are tested by the transient plane source (TPS) method. Correlations of thermal conductivity between unfrozen and frozen soil has been analyzed and recognized. Based on the measurement data of unfrozen soil thermal conductivity, the prediction models of frozen soil thermal conductivity for 7 typical soils in the QTEC are proposed. To further facilitate engineering applications, the prediction models of two soil categories (coarse and fine-grained soil) have also been proposed. The results demonstrate that, compared with nonideal prediction accuracy of using water content and dry density as the fitting parameter, the ternary fitting model has a higher thermal conductivity prediction accuracy for 7 types of frozen soils (more than 98% of the soil specimens' relative error are within 20%). The SVR model can further improve the frozen soil thermal conductivity prediction accuracy and more than 98% of the soil specimens' relative error are within 15%. For coarse and fine-grained soil categories, the above two models still have reliable prediction accuracy and determine coefficient (R^2) ranges from 0.8 to 0.91, which validates the applicability for small sample soils. This study provides feasible prediction models for frozen soil thermal conductivity and guidelines of the thermal design and freeze-thaw damage prevention for engineering structures in cold regions.

1. Introduction

With the increasing frequency of human activities and the trend of global warming, the temperature sensitive permafrost is changing significantly, most of which are in critical equilibrium state or even gradual degradation [1–3]. The widely distributed permafrost in the Qinghai-Tibet Plateau exhibits stronger temperature sensitivity and faster temperature rise rate than other permafrost regions with the same latitude [4–6]. The dynamic degradation process of frozen soil has a great impact on the stability of buildings in cold regions [7–10]. In the meanwhile, it will also lead to local environmental degradation, or further affect the global climate carbon cycle and climate change [11–14]. Therefore, many researchers had investigated the distribution, stability, and thermal regime of permafrost [15–17]. The thermal conductivity is one of the important thermophysical parameters for reconstructing the past and predicting the temperature status of permafrost under climate change conditions and also determining a parameter for engineering design in cold regions [18, 19]. Therefore, the

comprehensive understanding of variation law of soil thermal conductivity is one of the important tasks in permafrost research.

Thermal conductivity is an inherent parameter to characterize the heat transfer performance of soil, which can usually be obtained by means of experimental test and prediction models [20–22]. The test of thermal conductivity can generally be divided into the steady-state method and transient method [23, 24]. Specifically, it includes steady-state comparison method, steady-state heat flow meter method, transient hot wire method, transient heat pulse method, and TPS method [25]. However, the disadvantages of the experimental test are usually strict technical requirements, long time consumption, and high cost, and sometimes limited test results cannot satisfy the needs of practical applications. Therefore, as reported [26, 27], many soil thermal conductivity prediction models had been proposed. Empirical models are usually based on statistical analysis of thermal conductivity experimental results and use water content, dry density, porosity, and other related soil properties as fitting parameters [28–31]. Kersten [28] analyzed the test results of 19 soil types and established the empirical formula of thermal conductivity using water content and dry density. Johansen [29] proposed the concept of normalized thermal conductivity and given the interpolation calculation model of soil thermal conductivity based on the relationship between normalized coefficient and soil saturation. Lu et al. [30] performed a series of thermo-TDR tests on twelve natural soils and proposed a linear prediction model across a wide range of soil moisture condition. Yan et al. [31] developed a generalized effective soil thermal conductivity model for soils of various textures from dry to saturation. Then, many scholars improved the model for wider applicability and higher prediction accuracy [32–35]. At the same time, many scholars have established theoretical predictive models of soil thermal conductivity based on specific physical theory and models [36–38]. Farouki [39] and Xu et al. [40], respectively, established the weighted calculation model and geometric average calculation formula based on the volume ratio and thermal conductivity of each component of the frozen soil on the basis of predecessors. Considering for the interactions among soil particle, water, and air of a soil unit cell, Haigh [41] derived a theoretical thermal conductivity model for sand soil. In recent years, with the maturity of machine learning and its advantages in dealing with complex nonlinear problems, many researchers had adopted it to the prediction of soil thermal conductivity [42, 43]. For instance, Bang et al. [44] investigated the application effect of linear regression and various machine learning methods in the prediction of thermal conductivity of compacted bentonite and verified the feasibility and superiority of the machine learning method in the prediction of the soil thermal conductivity.

Compared to unfrozen soil, the specimen preparation and experimental procedures of frozen soil thermal conductivity testing are more complex and challengeable. And it can be found that the prediction accuracy of the frozen soil thermal conductivity predictive model is lower than that of unfrozen soil [40]. Meanwhile, as a complex multiphase composition, previous research indicated that the thermal conductivity of frozen soil was associated with many factors [26, 27, 45].The existing frozen soil thermal conductivity empirical model (usually using dry density, water content, porosity, etc., as the fitting parameters) cannot comprehensively consider the influences of complex multiphase and porous structural characteristics of soil. Therefore, in the present work, prediction models of frozen soil thermal conductivity using nonlinear regression and SVR methods have been developed considering for essentially multiphase and porous structural characteristic information reflection of unfrozen soil thermal conductivity. Thermal conductivity of various types of soil samples which are sampled from the QTEC are tested by the TPS method. Correlation analysis of thermal conductivity of unfrozen and frozen soil has been adopted. Based on the measurement data of unfrozen soil thermal conductivity, the ternary fitting and SVR prediction models of frozen soil thermal conductivity for the typical soils in the QTEC are proposed. To further facilitate engineering applications, the prediction models of coarse and fine-grained soil categories have been proposed. Furthermore, the prediction models of two soil categories have also been used to predict the frozen soil thermal conductivity of small size soil samples in the QTEC.

2. Materials and Methods

2.1. Soil Sample

2.1.1. Collection of Soil Samples. The soil samples of thermal conductivity measurement were collected from the drilling specimens of Qinghai-Tibet expressway geological exploration project, which was implemented by the CCCC First Highway Consultants Co. Ltd. and Eco-Environment and Resources Northwest Institute of CAS from September 2017 to June 2018. As shown in Figure 1, the sampling spot mainly locates in the permafrost regions between Xidatan and Tanggula Mountain (the corresponding Qinghai-Tibet Highway mileage is K2870~K3307). Every drilling spot is sampled for different depths, and the sampling depth varies from 0.5 m to 40 m. Total number of 638 unfrozen soil samples and 860 frozen soil samples are tested.

Soil types of testing specimens are determined by the classification criteria of geotechnical engineering. Figure 2 shows the statistic results of different types of soil samples (only numbers more than 15 are given). It can be seen that silty clay is the most widely distributed frozen soil type in the QTEC, and the following soil types are sandy and gravel soil. Because some soil samples with large water (ice) content are impossible to implement unfrozen soil thermal conductivity testing, a total of 609 specimens tested for both frozen and unfrozen are selected as the research objects in this work, and the statistical distribution of various soil samples is shown in Table 1. It can be seen that the proportions of silty clay, silt, fine sand, gravel sand, boulder, breccia, and all weathered rock soils accounting for 86.2% are defined as the typical analytical soil types in the following predictive model research.

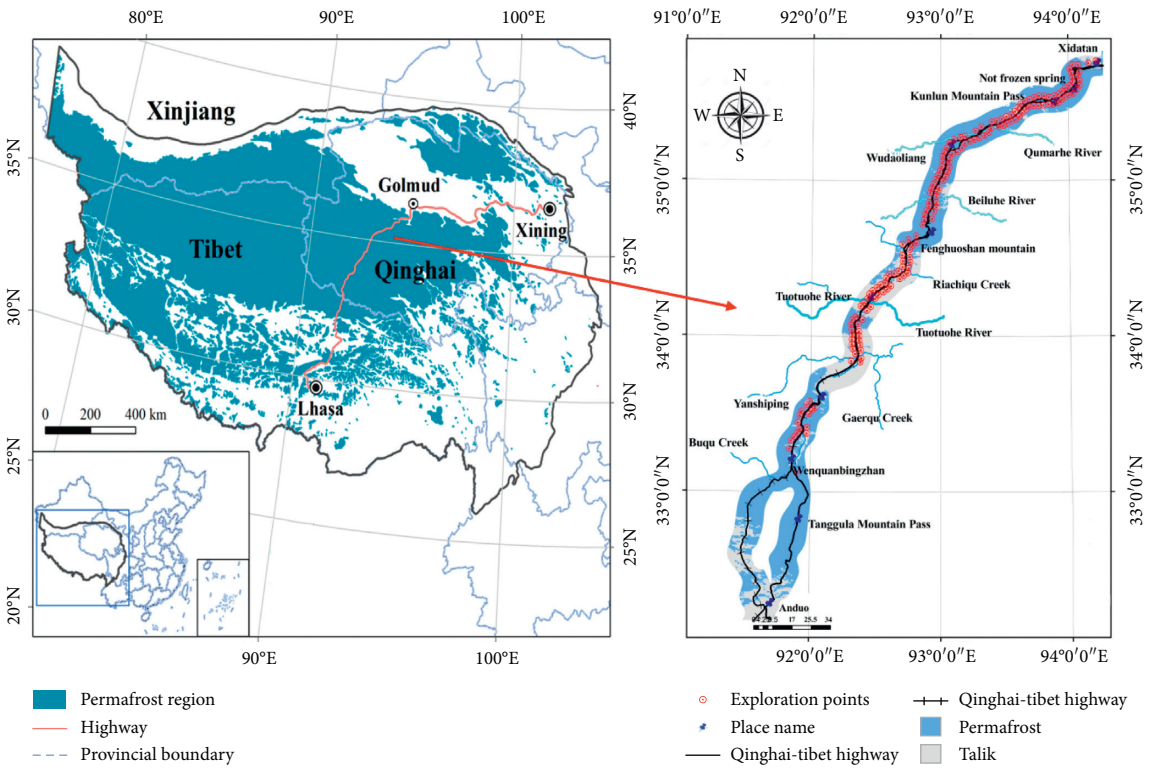

Figure 1: Schematic of the sampling spot along the QTEC [16].

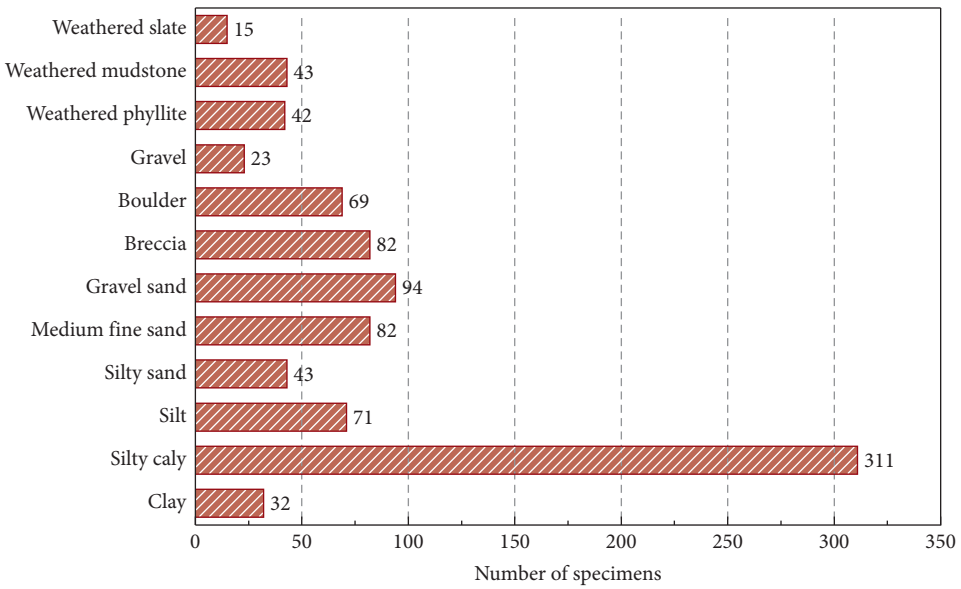

Figure 2: Statistic numbers of test samples for certain soil type.

2.1.2. Water Content and Dry Density Distribution of Soil Samples. The dry density (ρ_d) and water content (w) of soil samples are statistically calculated, and the accumulative proportion distribution is shown in Figure 3. It shows that the water content and dry density distributions are significantly correlated with soil properties. The dry density is negatively correlated with soil particle size and basic orders of dry density of the samples are silt, silty clay, weathered rock, fine sand, gravel sand, breccia, and boulder soils. The average dry density of above soil samples are 1.64, 1.69, 1.79, 1.83, 1.87, 1.92, and 2.06 g/cm^3, and the main distribution intervals (proportion within 10%~90%) are 1.40~1.81, 1.47~1.91, 1.53~2.04, 1.61~2.03, 1.66~2.15, 1.66~2.20, and 1.81~2.31 g/cm^3. Likewise, the orders of water content are silty clay, silt, weathered rock, fine sand, breccia, gravel sand, and boulder. The corresponding average values are 19.33%, 19.05%, 16.04%, 13.27%, 10.88%, 10.66%, and 9.28%, and main distribution interval are 11.68%~26.7%, 11.03%~

Table 1: Statistical distribution of various soil specimens.

Soil type		Numbers	Proportion (%)	Sampling depth (m)				
				≤1	1~5	5~10	10~20	≥20
Fine-grained soil	Clay	24	3.94	1	6	3	9	5
	Silty clay	202	33.17	10	63	40	69	20
	Silt	52	8.54	6	23	10	8	5
	Weathered slate	10	1.64	2	4	1	2	1
	Weathered phyllite	29	4.76	0	7	10	10	2
	Weathered sandstone	6	0.99	0	4	0	1	1
	Weathered marl	5	0.82	0	1	2	1	1
	Weathered mudstone	23	3.78	0	7	5	11	0
Coarse-grained soil	Silty sand	23	3.78	1	10	4	6	2
	Fine sand	49	8.05	14	19	9	2	5
	Medium sand	5	0.82	0	1	3	1	0
	Coarse sand	3	0.49	0	3	0	0	0
	Gravel sand	45	7.39	5	28	5	5	2
	Boulder	49	8.05	3	31	5	5	5
	Breccia	55	9.03	7	32	6	8	2
	Gravel + pebble	10	1.64	0	4	1	3	2
	Gravel soil	19	3.12	1	12	1	5	0

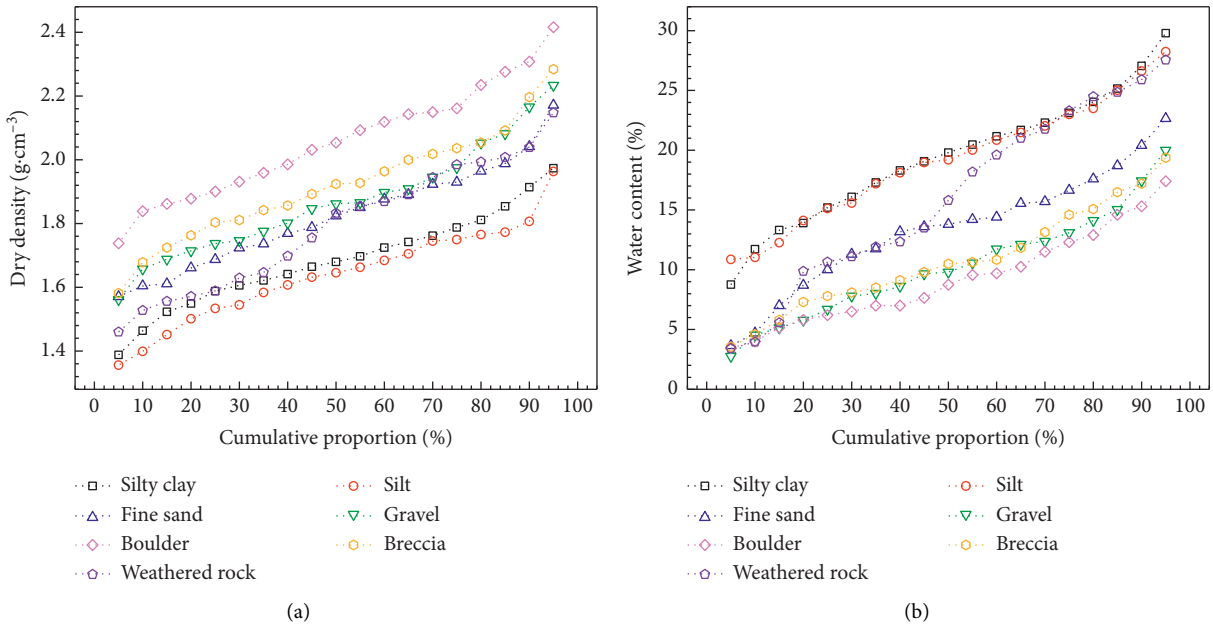

Figure 3: (a) Dry density and (b) water content probability distribution of soil samples.

26.62%, 3.96%~25.9%, 4.7%~20.16%, 4.6%~17.4%, 4.66%~18.64%, and 4%~15.2%, respectively, which basically covers all the water content ranges from dry to saturated.

2.2. Experimental Methods and Apparatus. The TPS method is utilized as the thermal conductivity testing measure for all soil samples. The experimental apparatus is the Hot Disk 1500s Thermal Conductivity Analyzer (as shown in Figure 4), which has ±3% measurement accuracy. The principle of the TPS method for measuring the thermal properties of materials is based on the transient temperature response of a step-heated disc-shaped heat source in an infinite medium. No. 4922 Kapton film probe with radius of 29.4 mm is used to make specimen as large as possible, and the thermal conductivity (λ) is calculated by line equation of temperature variation values and dimensionless time constant which is measured by the film sensor:

$$\Delta\overline{T}(\tau) = \frac{P_0}{\pi^{3/2} r\lambda} D(\tau), \quad (1)$$

where $\Delta\overline{T}(\tau)$ is the temperature variation value, P_0 is the total output of power and r is the radius of Kapton film sensor, and $D(\tau)$ is the dimensionless time constant. During the test, experimental soil samples are formed into 3 cm height and 8 cm diameters column, and the film probe is

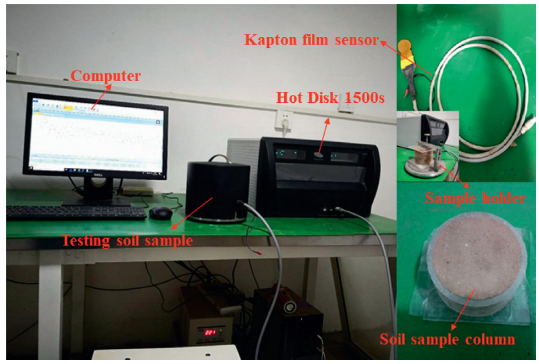

Figure 4: Thermal conductivity test system.

sandwiched between two soil samples and fixed with a stainless steel sample holder. The detailed experimental procedures can be obtained in our previous work [46].

2.3. Nonlinear Regression Model. Previous studies have shown that dry density and water content have significant influence on soil's thermal conductivity. Partial correlation analysis between frozen soil thermal conductivity of dry density, water content, and unfrozen soil thermal conductivity for two soil categories have been performed, and the results are shown in Table 2. The results exhibit that dry density and water content, as well as unfrozen soil thermal conductivity (λ_u), have significant positive correlations with frozen soil thermal conductivity (λ_f). In particular, it should be noted that the correlation between the frozen and unfrozen soil thermal conductivity for both coarse and fine-grained soils are very high (0.88 and 0.93, respectively). It can be inferred that, considering for the essential soil properties information reflection of unfrozen soil thermal conductivity, it would be possible to utilize the unfrozen soil thermal conductivity to predict frozen soil thermal conductivity.

Curve estimation of the fitting relationship between the frozen soil thermal conductivity and three factors has been taken, and it is found that the thermal conductivity of the frozen soil is linear with the unfrozen soil thermal conductivity, while its relation with dry density and water content are in the form of logarithmic functions. The ternary fitting formulas of frozen soil thermal conductivity for 7 typical soils in the QTEC are given as follows:

$$\lambda_f = a + b\lambda_u + c\ln(w) + d\ln(\rho_d), \tag{2}$$

where a, b, c, and d are the fitting coefficients of the equation. The detail fitting results of 7 typical soils are listed in Table 3. It can be seen that the determine coefficients (R^2) of 7 typical soils range from 0.76~0.93, while the analog effect of sandy soils are better than other soil types.

In order to analysis the predictive effect of the ternary fitting model, the estimated frozen soil thermal conductivity based on the Kersten model [28], Gangadhara Rao and Singh model [47], and ternary fitting model are plotted against the measured value of testing dataset. The empirical formulas proposed by Kersten and Gangadhara Rao and Singh used dry density and water content as fitting parameters, while the applicable soil types are silt, fine sand and gravel sand soils, etc. The comparison results of the estimation values of three models and the experimental values are shown in Figure 5. It can be seen that the proposed ternary fitting model performs best among all three models as most of the predictive values are within the ±10% relative error line. However, the predictive values of Kersten and Gangadhara Rao and Singh models are generally overestimated for all soil types and their prediction errors reach up to 40%. Therefore, it can be concluded that, compared with nonideal prediction accuracy of binary fitting models, the ternary fitting model using the unfrozen soil thermal conductivity as the fitting parameter has a higher thermal conductivity prediction accuracy.

3. Development of SVR Models

3.1. Theory and Performance Evaluation of SVR Model. SVR method is a type of supervised machine learning method and proposed by Vapnik et al. [48, 49], which is based on statistical learning theory. The SVR method uses kernel functions to map low-dimensional nonlinear problems to high-dimensional space to achieve linear separability and then to seek linear regression equations to fit sample data (as shown in Figure 6). The regression function can be expressed as follows:

$$f(x) = K^T\varphi(x) + m, \tag{3}$$

where x is the input vector, K is the weight vector, m is the offset vector, and $\varphi(x)$ is eigenvector that maps input data to the high-dimensional space. The Gaussian radial basis function is chosen as the kernel function in the calculation.

The SVR method is based on the principle of minimizing structural risk, transforming the linear regression problem into the following optimization problem, and then the values of K and m can be determined [48]:

$$\begin{aligned} &\text{Minimize} \quad \frac{1}{2}K^TK + t\sum_{i=1}^{n}(\xi_i + \xi_i^*), \\ &\text{Subject to} \quad \begin{cases} y_i - K^T\varphi(x) - m \le \varepsilon + \xi_i \\ K^T\varphi(x) + m - y_i \le \varepsilon + \xi_i^* \\ \xi_i, \xi_i^* \ge 0, \end{cases} \end{aligned} \tag{4}$$

where t is the penalty parameter which is greater than 0, ε is the insensitive loss coefficient, and ξ_i and ξ_i^* are slack variables.

The predictive results of SVR models for silt and gravel sand soils are shown in Figure 7. It can be seen that the predictive results of the SVR model are in good agreement with the experimental results ($R^2 = 0.86$ for silt and $R^2 = 0.94$ for gravel sand). The SVR model exhibits remarkable prediction accuracy and most of predictive values are within the ±10% error bars, which validates their predictive availability

Table 2: Partial correlation analysis between frozen soil thermal conductivity, dry density, water content, and unfrozen soil thermal conductivity.

Soil categories	Related variables	Control variables	Unfrozen soil thermal conductivity	Frozen soil thermal conductivity
Fine-grained soil	Water content	Dry density	0.312	0.450
	Unfrozen soil thermal conductivity		—	0.880
	Dry density	Water content	0.456	0.385
	Unfrozen soil thermal conductivity		—	0.891
Coarse-grained soil	Water content	Dry density	0.501	0.608
	Unfrozen soil thermal conductivity		—	0.927
	Dry density	Water content	0.530	0.502
	Unfrozen soil thermal conductivity		—	0.930

Table 3: Ternary fitting result of frozen soil thermal conductivity for 7 typical soils in the QTEC.

Soil type	Fitting coefficients				R^2
	a	b	c	d	
Silty clay	−0.703	1.291	0.238	0.007	0.759
Silt	−1.358	1.283	0.424	0.248	0.792
Weathered rock	−0.102	1.370	0.183	−0.854	0.895
Fine sand	−0.220	1.290	0.146	−0.429	0.908
Gravel sand	−0.617	1.272	0.254	−0.138	0.933
Boulder	−1.257	1.049	0.497	0.702	0.865
Breccia	−1.282	0.884	0.459	1.239	0.78

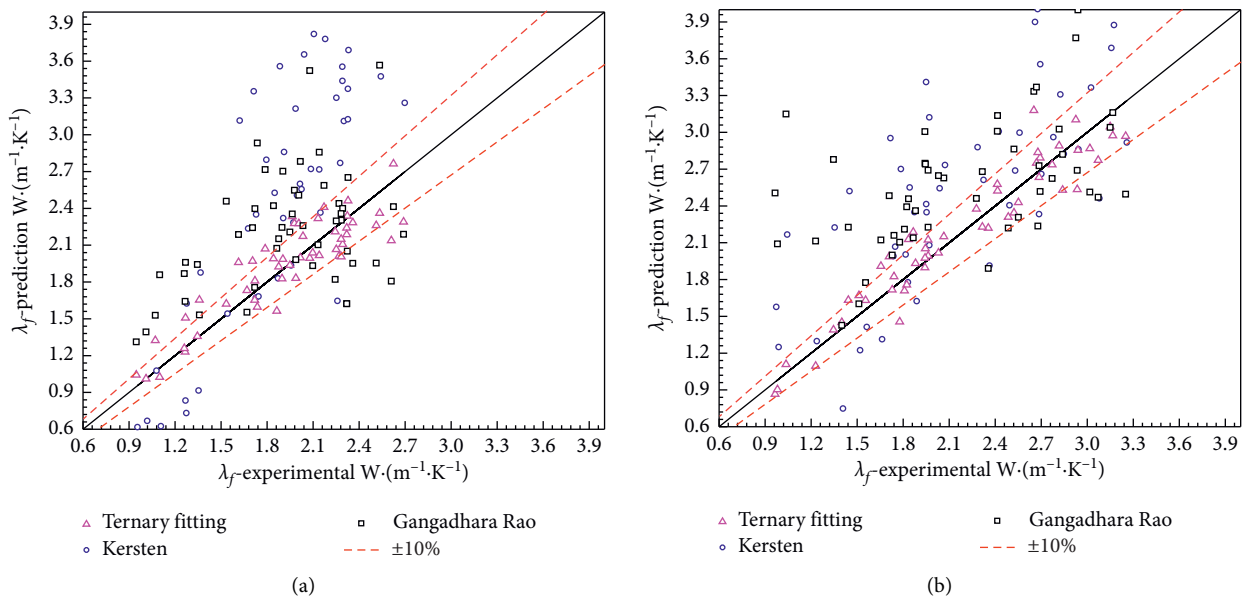

Figure 5: Continued.

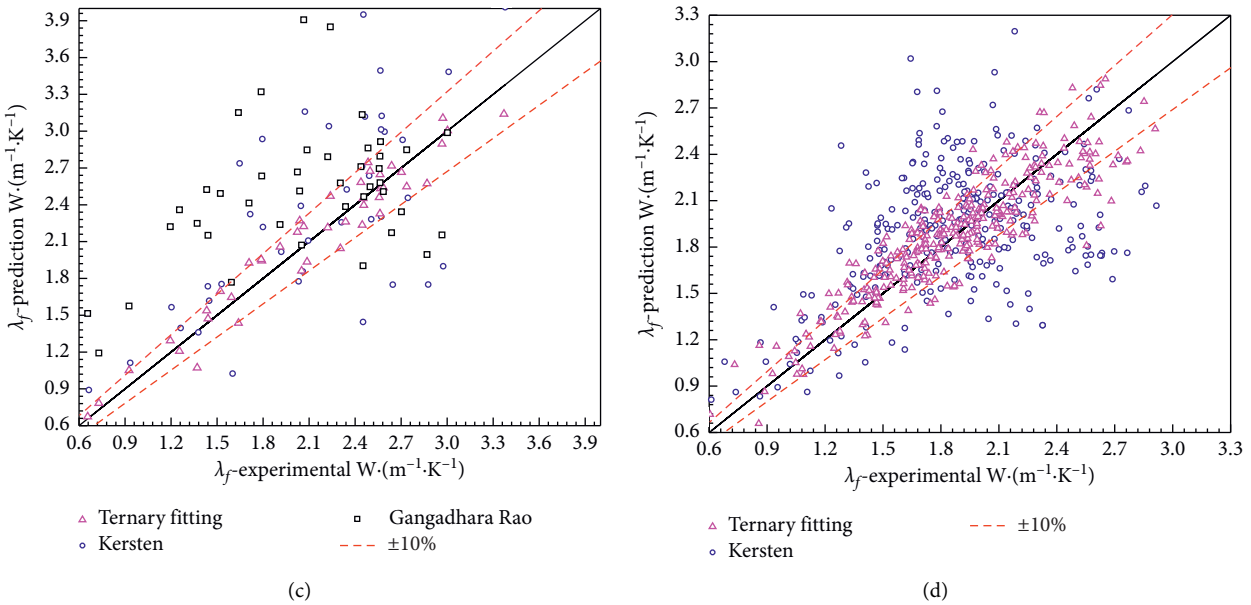

Figure 5: A comparison of measured and estimated frozen soil thermal conductivity. (a) Slit. (b) Fine sand. (c) Gravel sand. (d) Fine-grained sand.

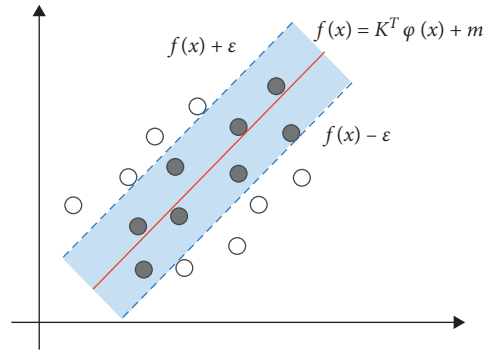

Figure 6: Schematic diagram of the SVR method.

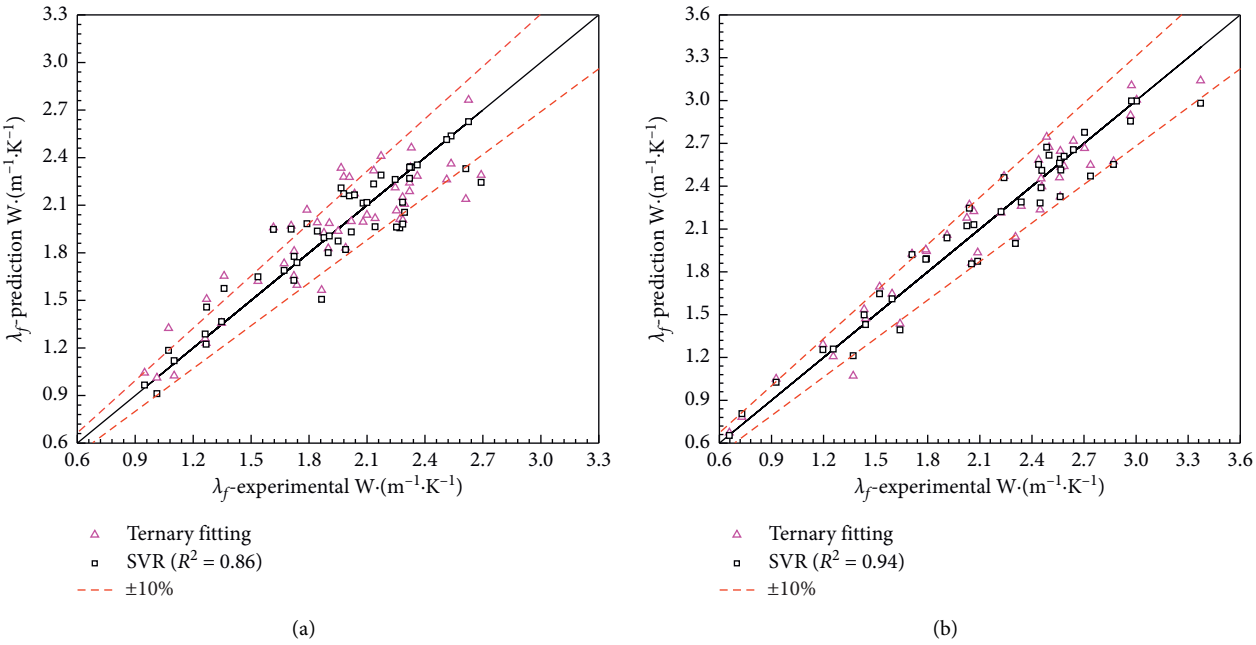

Figure 7: Predictive results of SVR models for (a) slit and (b) gravel sand.

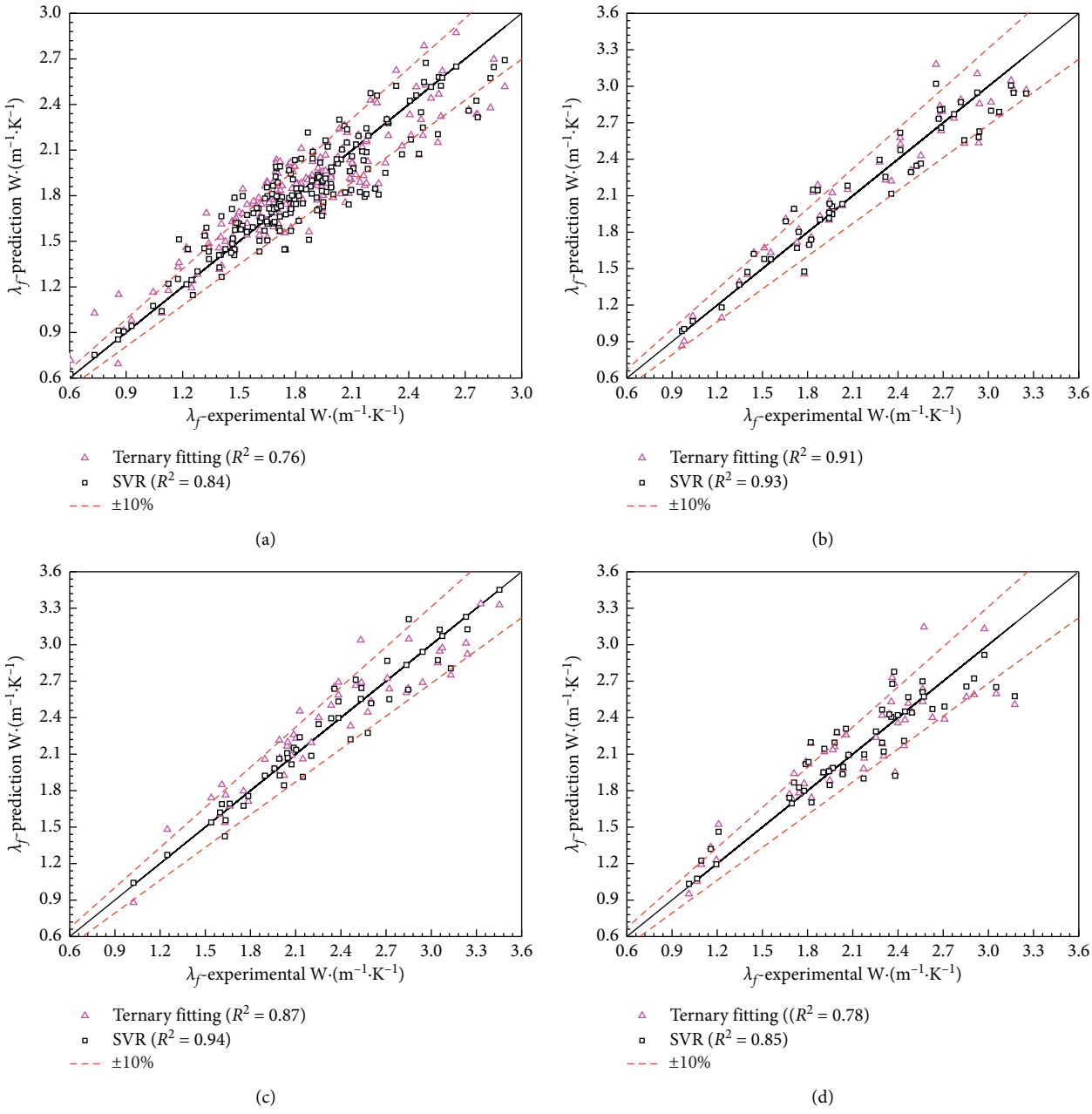

Figure 8: Comparison of predictive results of the SVR model and ternary fitting model. (a) Slit. (b) Fine sand. (c) Boulder. (d) Breccia.

and engineering suitability. Furthermore, it also should be noted that evaluation spots in Figure 7 is distributed uniformly throughout the thermal conductivity interval (λ_f ranges 0.6~3.3 W/(m·K)), which proves the broader application range of the SVR model.

3.2. Comparison of SVR Model with Ternary Fitting Model. The comparison of predictive results of the SVR model and ternary fitting model are shown in Figure 8. It can be seen that the fitting degree of the SVR model is much higher than that of the ternary fitting model. Especially for the silty clay and breccia soils, the predictive improvement effect of the SVR method is more obvious. For improvement at both high and low thermal conductivity intervals, the R^2 increases to 0.84 and 0.85, respectively. It can be considered that, for the complex multiphase and porous structural characteristics of soil, the SVR model has more advantages than the traditional empirical formula model.

The fitting results of the ternary fitting method and SVR method are statistically calculated. The distributions of R^2, sample probability of mean absolute percent error (MAPE) less than 10%, and maximum relative error (δ_{max}) are shown in Table 4. It can be seen that, compared with ternary fitting method, the minimum R^2 of the SVR method is 0.84 (silty clay), and the R^2 of 4 soil types is above 0.9. The 7 typical soils' average δ_{max} of the SVR model is 18.1% and ternary fitting model is 21.9%. Moreover, the proportion of MAPE

Table 4: Statistics of prediction results of the ternary fitting model and SVR model.

Predictive model	Statistical values	Silty clay	Silt	Weathered rock	Fine sand	Gravel sand	Boulder	Breccia
Ternary fitting method	R^2	0.76	0.79	0.9	0.91	0.93	0.87	0.78
	MAPE ≤ 10%	63.30%	68%	76.36%	76%	76.74%	77.08%	65.38%
	δ_{max}	26.6%	22.88%	16.78%	19.62%	22.11%	19.73%	25.3%
SVR model	R^2	0.84	0.86	0.91	0.92	0.94	0.94	0.85
	MAPE ≤ 10%	74.74%	83.64%	72.55%	78.43%	79.07%	83.33%	69.81%
	δ_{max}	20.47%	19.89%	19.62%	17.49%	15.62%	13.23%	20.04%

Table 5: Fitting results of coarse and fine-grained soil categories.

Soil type	Ternary fitting					SVR
	a	b	c	d	R^2	R^2
Fine-grained soil	−0.770	1.355	0.253	−0.102	0.80	0.85
Coarse-grained soil	−0.788	1.190	0.293	0.225	0.89	0.91

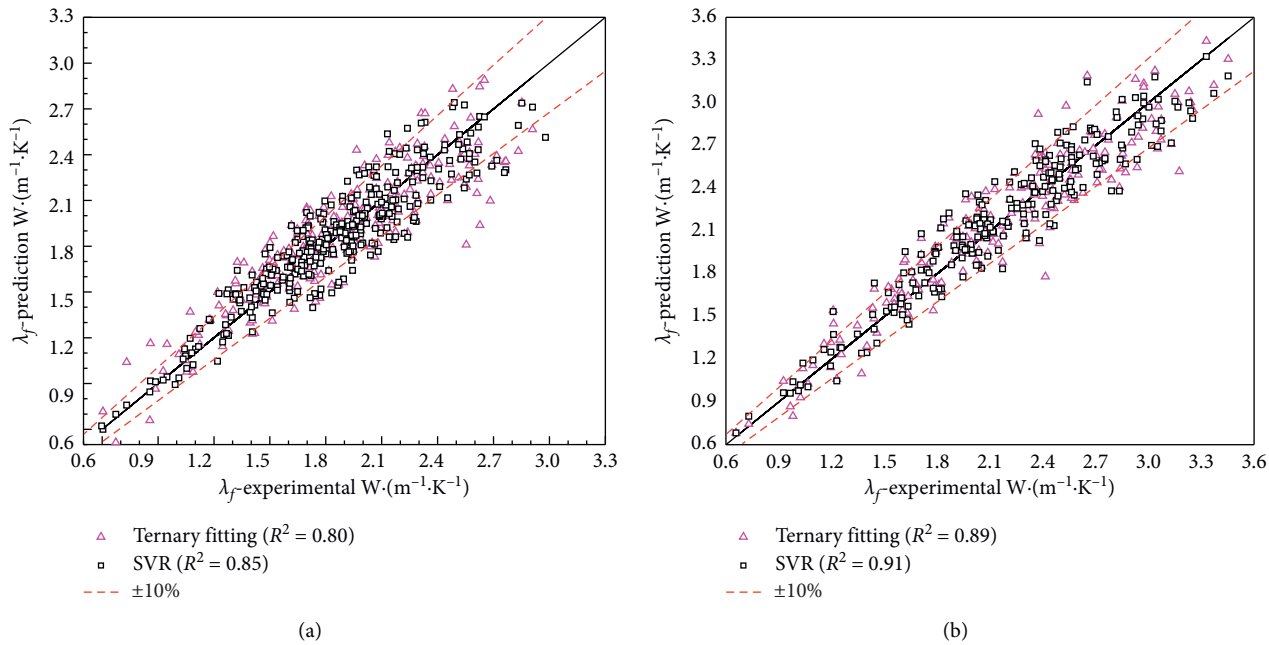

Figure 9: Comparison of predictive results of ternary fitting and SVR models for (a) fine-grained sand and (b) coarse-grained sand.

less than 10% of SVR model are larger than that of ternary fitting model for all 7 typical soils, which further indicate that the SVR model has better performance than the ternary fitting model. The sample probability of the MAPE within 20% of the ternary fitting method is more than 98%, while the sample probability of the MAPE within 15% of the SVR method is more than 98%. Therefore, it can be considered that the ternary fitting method has a predictive accuracy of ±20% and the SVR method has a predictive accuracy of ±15%.

4. Generalized Prediction Model for Coarse and Fine-Grained Soil

Based on the previous analysis, it can be found that some soil types, such as clay, silty sand, and gravel soil, cannot be analyzed by the nonlinear regression or SVR method for their small sample sizes. Furthermore, the overly detailed prediction models of subdivided soil types will also induce a certain degree of inconvenience in engineering application. Thus, generalized frozen soil thermal conductivity prediction models for coarse and fine-grained soil categories have been developed. The R^2 and fitting coefficient values of the ternary fitting model and SVR model are listed in Table 5, and the comparison of predictive results of the above two models for coarse and fine-grained soil categories are shown in Figure 9. It shows that both the ternary fitting model and SVR model have acceptable fitting effect for two soil categories, and most evaluation spots of two models are within or near the ±10% error. The R^2 of the ternary fitting model for the coarse and fine-grained soil categories is 0.80 and 0.89, respectively, while the SVR model is 0.85 and 0.91, which proves the feasibility of soil categories predictive models. Nevertheless, it also can be found that the SVR

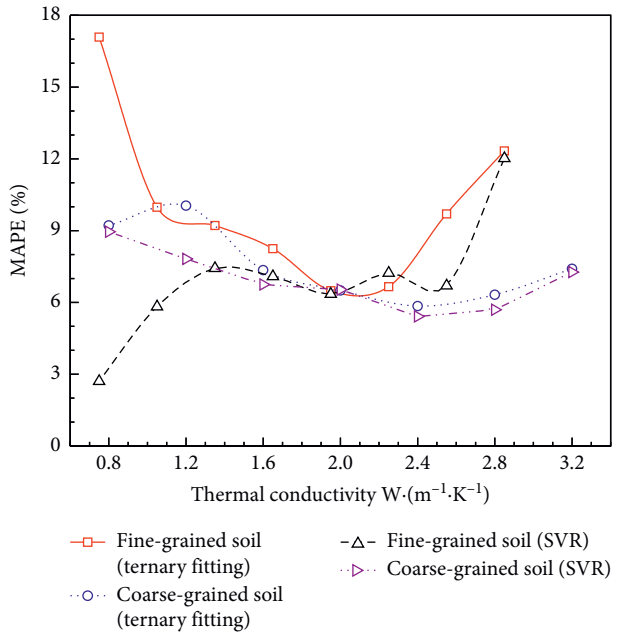

Figure 10: MAPE distribution of ternary fitting and SVR models for coarse- and fine-grained soil categories.

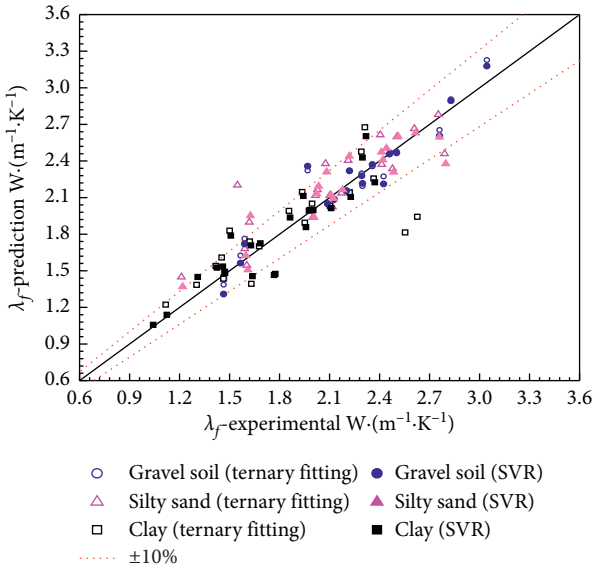

Figure 11: Prediction results of small sample soils.

method still has a better performance despite the increase of variety and complexity of soil samples.

The MAPE distribution of two prediction models of coarse- and fine-grained soil categories is shown in Figure 10. It can be seen that the prediction accuracy of coarse-grained soil category is generally higher than that of fine-grained soil category. The MAPE of coarse-grained soil category distributes uniformly in each thermal conductivity range and its average value is lower than 10%, which means that the predictive results of two prediction models for coarse-grained soil category are more reliable in the entire frozen soil thermal conductivity distribution interval. Additionally, it should be mentioned that the large error intervals of fine-grained soil category are mainly concentrated in 0~1.2 W/(m·K) and 2.7~3.6 W/(m·K) ranges and the proportion of the two ranges are 6.67% and 2.6% (total of 9.27%), which is roughly excluded from its main thermal conductivity distribution range. Therefore, considering for applicability scope and convenience, the fine-grained soil category prediction models definitely have certain application values in engineering.

The prediction models of two soil categories are applied to small sample soils (clay, silty sand, and gravel soil), and the results are shown in Figure 11. It can be seen that both ternary fitting model and SVR model exhibit good predictive accuracy for all three small sample soils, which supports applicability of prediction models. Furthermore, it can be clearly noted that the SVR model has better predictive performance for clay soil, which testify that the machine learning method has broad application prospects for its capability of nonlinear and complex relationship capturing and imitating.

5. Conclusions

In present work, a large-scale soil thermal conductivity test has been conducted by the TPS method. Correlation analysis of thermal conductivity of unfrozen and frozen soil has been adopted. Based on the measurement data of unfrozen soil thermal conductivity, the ternary fitting and SVR prediction models of frozen soil thermal conductivity for the typical soils in the QTEC are proposed considering for the essential soil properties information reflection of unfrozen soil thermal conductivity. Furthermore, to facilitate engineering applications, the prediction models of coarse and fine-grained soil categories have also been proposed and compared. The results show that

(1) Compared with nonideal prediction accuracy of using water content and dry density as the fitting parameter, the ternary fitting model has a higher thermal conductivity prediction accuracy for typical soil types in QTEC, and more than 98% of soil specimens' relative error are within 20%

(2) With the capability of nonlinear and complex relationship capturing and imitating, the SVR model can further improve the frozen soil thermal conductivity prediction accuracy and more than 98% of the soil specimens' relative error are within 15%

(3) For coarse- and fine-grained soil categories, the above ternary fitting and SVR models still have reliable prediction accuracy and their R^2 ranges from 0.8 to 0.91, which validates the applicability for small sample soils

Data Availability

All the data used to support the findings of this study are available from the corresponding author upon request.

Conflicts of Interest

The authors declare that they have no conflicts of interest.

Acknowledgments

This research was supported by the National Science Foundation of China (Grant nos. 41502292 and 51574037), Applied Fundamental Research Project of China Communications Construction Co., Ltd. (nos. 2018-ZJKJ-PTJS03 and 2016-ZJKJ-02), and project funded by China Postdoctoral Science Foundation (no. 2014M560739).

References

[1] G. Doré, F. Niu, and H. Brooks, "Adaptation methods for transportation infrastructure built on degrading permafrost," *Permafrost and Periglacial Processes*, vol. 27, no. 4, pp. 352–364, 2016.

[2] Y. Ding, S. Zhang, L. Zhao, Z. Li, and S. Kang, "Global warming weakening the inherent stability of glaciers and permafrost," *Science Bulletin*, vol. 64, no. 4, pp. 245–253, 2019.

[3] Y. Ran, X. Li, and G. Cheng, "Climate warming over the past half century has led to thermal degradation of permafrost on the Qinghai-Tibet Plateau," *The Cryosphere*, vol. 12, no. 2, pp. 595–608, 2018.

[4] S. Chen, X. F. Li, and T. H. Wu, "Soil thermal regime alteration under experimental warming in permafrost regions of the central Tibetan Plateau," *Geoderma*, vol. 372, Article ID 114397, 2020.

[5] Z. Q. Zhang, Q. B. Wu, G. L. Jiang, S. R. Gao, J. Chen, and Y. Z. Liu, "Changes in the permafrost temperatures from 2003 to 2015 in the Qinghai-Tibet Plateau," *Cold Regions Science and Technology*, vol. 169, Article ID 102904, 2020.

[6] T. Wang, T. Wu, P. Wang, R. Li, C. Xie, and D. Zou, "Spatial distribution and changes of permafrost on the Qinghai-Tibet Plateau revealed by statistical models during the period of 1980 to 2010," *Science of The Total Environment*, vol. 650, no. 1, pp. 661–670, 2019.

[7] F. E. Nelson, O. A. Anisimov, and N. I. Shiklomanov, "Subsidence risk from thawing permafrost," *Nature*, vol. 410, no. 6831, pp. 889-890, 2001.

[8] J. Hjort, O. Karjalainen, J. Aalto et al., "Degrading permafrost puts Arctic infrastructure at risk by mid-century," *Nature Communications*, vol. 9, no. 1, Article ID 5147, 2018.

[9] Y. J. Shen, Y. Z. Wang, X. Wei, H. L. Jia, and R. X. Yan, "Investigation on meso-debonding process of the sandstone–concrete interface induced by freeze–thaw cycles using NMR technology," *Construction and Building Materials*, vol. 252, Article ID 118962, 2020.

[10] Y. J. Shen, X. Hou, J. Q. Z. H. Yuan et al., "Thermal deterioration of high-temperature granite after cooling shock: multiple-identification and damage mechanism," *Bulletin of Engineering Geology and the Environment*, vol. 7, pp. 1–14, 2020.

[11] M. X. Yang, F. E. Nelson, N. I. Shiklomanov, D. L. Dong, and G. N. Wan, "Permafrost degradation and its environmental effects on the Tibetan Plateau: a review of recent research," *Earth-Science Reviews*, vol. 103, no. 1-2, pp. 31–44, 2010.

[12] M. R. Turetsky, B. W. Abbott, M. C. Jones et al., "Permafrost collapse is accelerating carbon release," *Nature*, vol. 569, no. 7754, pp. 32–34, 2019.

[13] E. A. G. Schuur, A. D. Mcguire, C. Schädel et al., "Climate change and the permafrost carbon feedback," *Nature*, vol. 520, no. 7546, pp. 171–179, 2015.

[14] M. Yang, X. Wang, G. Pang, G. Wan, and Z. Liu, "The Tibetan Plateau cryosphere: observations and model simulations for current status and recent changes," *Earth-Science Reviews*, vol. 190, pp. 353–369, 2019.

[15] Q. Z. Wang, J. H. Fang, X. Q. Zhao, and K. Hu, "The influence of pavement type on the thermal stability of block-stone embankments in the warm permafrost region," *Transportation Geotechnics*, vol. 23, Article ID 100334, 2020.

[16] M. Zhang, Y. Lai, Q. Wu et al., "A full-scale field experiment to evaluate the cooling performance of a novel composite embankment in permafrost regions," *International Journal of Heat and Mass Transfer*, vol. 95, pp. 1047–1056, 2016.

[17] Z. Y. Liu, F. Q. Cui, J. B. Chen, L. Jin, W. Wang, and W. Zhang, "Study on the permafrost heat transfer mechanism and reasonable interval of separate embankment for the Qinghai-Tibet expressway," *Cold Regions Science and Technology*, vol. 170, Article ID 102952, 2020.

[18] Y. J. Shen, H. W. Yang, J. M. Xi, Y. Yang, Y. Z. Wang, and X. Wei, "A novel shearing fracture morphology method to assess the influence of freeze–thaw actions on concrete–granite interface," *Cold Regions Science and Technology*, vol. 169, Article ID 102900, 2020.

[19] Y. Zhang, W. Chen, and D. W. Riseborough, "Transient projections of permafrost distribution in Canada during the 21st century under scenarios of climate change," *Global and Planetary Change*, vol. 60, no. 3-4, pp. 443–456, 2008.

[20] A. Alrtimi, M. Rouainia, and S. Haigh, "Thermal conductivity of a sandy soil," *Applied Thermal Engineering*, vol. 106, pp. 551–560, 2016.

[21] R. Li, L. Zhao, T. Wu et al., "Soil thermal conductivity and its influencing factors at the Tanggula permafrost region on the Qinghai-Tibet Plateau," *Agricultural and Forest Meteorology*, vol. 264, pp. 235–246, 2019.

[22] Y. Z. Du, R. Li, L. Zhao et al., "Evaluation of 11 soil thermal conductivity schemes for the permafrost region of the central Qinghai-Tibet Plateau," *Catena*, vol. 193, Article ID 104608, 2020.

[23] D. Barry-Macaulay, A. Bouazza, R. M. Singh, B. Wang, and P. G. Ranjith, "Thermal conductivity of soils and rocks from the Melbourne (Australia) region," *Engineering Geology*, vol. 164, pp. 131–138, 2013.

[24] G. Cai, T. Zhang, A. J. Puppala, and S. Liu, "Thermal characterization and prediction model of typical soils in Nanjing area of China," *Engineering Geology*, vol. 191, pp. 23–30, 2015.

[25] X. Zhao, G. Zhou, and X. Jiang, "Measurement of thermal conductivity for frozen soil at temperatures close to 0°C," *Measurement*, vol. 140, pp. 504–510, 2019.

[26] N. Zhang, Z. Wang, S. Q. Xia, and X. Y. Hou, "Review of soil thermal conductivity and predictive models," *International Journal of Thermal Sciences*, vol. 117, pp. 172–183, 2017.

[27] Y. Dong, J. S. McCartney, and N. Lu, "Critical review of thermal conductivity models for unsaturated soils," *Geotechnical and Geological Engineering*, vol. 33, no. 2, pp. 207–221, 2015.

[28] M. S. Kersten, *Laboratory Research for the Determination of the Thermal Properties of Soils*, University of Minnesota, Minneapolis, MN, USA, 1949.

[29] O. Johansen, *Thermal Conductivity of Soils*, Trondheim University, Trondheim, Norway, 1975.

[30] S. Lu, T. Ren, Y. Gong, and R. Horton, "An improved model for predicting soil thermal conductivity from water content at

room temperature," *Soil Science Society of America Journal*, vol. 71, no. 1, pp. 8–14, 2007.

[31] H. Yan, H. He, M. Dyck et al., "A generalized model for estimating effective soil thermal conductivity based on the Kasubuchi algorithm," *Geoderma*, vol. 353, pp. 227–242, 2019.

[32] J. Côté and J.-M. Konrad, "A generalized thermal conductivity model for soils and construction materials," *Canadian Geotechnical Journal*, vol. 42, no. 2, pp. 443–458, 2005.

[33] S. Q. Luo, S. H. Lu, Y. Zhang et al., "Soil thermal conductivity parameterization establishment and application in numerical model of central Tibetan Plateau," *Chinese Journal of Geophysics*, vol. 52, no. 4, pp. 338-339, 2009.

[34] N. Zhang, X. B. Yu, A. Pradhan, and A. J. Puppala, "Thermal conductivity of quartz sands by thermo-time domain reflectometry probe and model prediction," *Journal of Materials in Civil Engineering*, vol. 27, no. 12, pp. 1–10, Article ID 04015059, 2015.

[35] V. Balland and P. A. Arp, "Modeling soil thermal conductivities over a wide range of conditions," *Journal of Environmental Engineering and Science*, vol. 4, no. 6, pp. 549–558, 2005.

[36] D. A. De Vries, "Thermal properties of soils," *Physics of the Plant Environment*, pp. 210–235, North-Holland Publishing Co., Amsterdam, Netherlands, 1963.

[37] F. Gori, "A theoretical model for predicting the effective thermal conductivity of unsaturated frozen soils," in *Proceedings of the 4th International Conference on Permafrost, Fairbanks*, pp. 363–368, Fairbanks, AK, USA, July 1983.

[38] F. Tong, L. Jing, and R. W. Zimmerman, "A fully coupled thermo-hydro-mechanical model for simulating multiphase flow, deformation and heat transfer in buffer material and rock masses," *International Journal of Rock Mechanics and Mining Sciences*, vol. 47, no. 2, pp. 205–217, 2010.

[39] O. T. Farouki, "The thermal properties of soils in cold regions," *Cold Regions Science and Technology*, vol. 5, no. 1, pp. 67–75, 1981.

[40] X. Z. Xu, J. C. Wang, and L. X. Zhang, *Frozen Soil Physics*, Science Press, Beijing, China, 2010.

[41] S. K. Haigh, "Thermal conductivity of sands," *Géotechnique*, vol. 62, no. 7, pp. 617–625, 2012.

[42] T. Zhang, C. J. Wang, S. Y. Liu, N. Zhang, and T. W. Zhang, "Assessment of soil thermal conduction using artificial neural network models," *Cold Regions Science and Technology*, vol. 169, Article ID 102907, 2019.

[43] N. Zhang, H. Zou, L. Zhang, A. J. Puppala, S. Liu, and G. Cai, "A unified soil thermal conductivity model based on artificial neural network," *International Journal of Thermal Sciences*, vol. 155, Article ID 106414, 2020.

[44] H. T. Bang, S. Yoon, and H. Jeon, "Application of machine learning methods to predict a thermal conductivity model for compacted bentonite," *Annals of Nuclear Energy*, vol. 142, Article ID 107395, 2020.

[45] J. Bi, M. Zhang, W. Chen, J. Lu, and Y. Lai, "A new model to determine the thermal conductivity of fine-grained soils," *International Journal of Heat and Mass Transfer*, vol. 123, pp. 407–417, 2018.

[46] F. Q. Cui, Z. Y. Liu, J. B. Chen, Y. H. Dong, L. Jin, and H. Peng, "Experimental test and prediction model of soil thermal conductivity in permafrost regions," *Applied Sciences*, vol. 10, no. 7, Article ID 2476, 2020.

[47] M. Gangadhara Rao and D. N. Singh, "A generalized relationship to estimate thermal resistivity of soils," *Canadian Geotechnical Journal*, vol. 36, no. 4, pp. 767–773, 1999.

[48] V. Vapnik, S. E. Golowich, and A. J. Smola, "Support vector method for function, approximation, regression estimation and signal processing," *Advances in Neural Information Processing Systems*, pp. 281–287, MIT Press, Cambridge, MA, USA, 1997.

[49] R. G. Brereton and G. R. Lloyd, "Support vector machines for classification and regression," *The Analyst*, vol. 135, no. 2, pp. 230–267, 2010.